



WP6 X-ray sensor trade-off

Doc. no. : AHEAD-WP6-REP-002-2016
Issue : 1.1
Date : 16 September 2016
Cat :
Page : 1 of 23

Title : **WP6: X-ray sensor trade-off**

Prepared by: Gao Jian-Rong Date: 16 September 2016
Roland den Hartog

Checked by: Jan-Willem den Herder Date: 16 September 2016

PA agreed by: Date:

Authorised by: Date:

Distribution

AHEAD WP6 leaders
AHEAD management team



WP6 X-ray sensor trade-off

Doc. no. : AHEAD-WP6-REP-002-2016

Issue : 1.1

Date : 16 September 2016

Cat :

Page : 2 of 23

Document Change Record:

Issue	Date	Changed Section	Description of Change
0.0	17 June 2016	All	First draft version
1.0	1 September 2016	All	Final version for the EU
1.1	16 September 2016	6	Updated numbering and clarified that the development of an array with a lower bandwidth (section 6.2) will be done with Ti/Au TESs



WP6 X-ray sensor trade-off

Doc. no. : AHEAD-WP6-REP-002-2016
Issue : 1.1
Date : 16 September 2016
Cat :
Page : 3 of 23

Contents

Applicable Documents.....	4
1 Introduction.....	6
2 Transition Edge Sensors for detecting X-rays.....	8
2.0 Detection principle	8
2.1 Spectral resolution	8
2.3 Count rate	9
3 Instrument requirements.....	11
4 Defocusing optics	13
4.1 Simpler array fabrication.....	14
4.2 Simpler array wiring	14
4.3 Relaxed readout requirements	14
4.4 Longer event lengths.....	14
4.5 Uniform calibration counts.....	14
4.6 Less (thermal) crosstalk.....	14
4.7 Relaxed pointing requirements.....	15
4.8 Uniform loading of readout chain.....	15
5 Sensor trade-off.....	17
6 Conclusions	21
6.1 Baseline TES array	21
6.2 TES array with lower bandwidth	21
6.3 Improved energy resolution.....	21



WP6 X-ray sensor trade-off

Doc. no. : AHEAD-WP6-REP-002-2016
Issue : 1.1
Date : 16 September 2016
Cat :
Page : 4 of 23

Applicable Documents

[AD#]	Doc. Reference	Issue	Title
AD1	AHEAD consortium agreement	15-06-2015, final version	Integrated Activities for the High-Energy Astrophysics Domain, consortium Agreement
AD2	AHEAD-PO-MIN-001/2015	15 September 2015	AHEAD Kick-Off meeting, Minutes of the Consortium Board meeting

Reference Documents

RD#	Doc. Reference	Issue	title
RD1	SRON-XIFU-TN-2015-017	0.3	Technical requirements review for CTP progress meeting 1
RD2	SRON-XIFU-TN-2015-010	0.7	Array configuration readout
RD3	SRON-XIFU-TN-2015-009	0.2	X-IFU sensor array configuration, phase 0 trade report
RD4	D. Barret et al.	Proc. SPIE 9905, July 2016	The Athena X-ray Integral Field Unit,
RD5	SRON-ATH-PL-2014-001	1 July 2015	Athena: Mock Observing Plan
RD6	SRON-XIFU-SP-2015-004	0.4, 15 June 2016	X-IFU Energy Resolution Budget
RD7	X-IFU-FPSDRAFT	23 June 2015	Focal Plane Study: Event Grading
RD8	S. Bandler et al.	TES-VI ASC meeting, Portland, 2012	Advances in small pixel TES-based X-ray microcalorimeter arrays for solar physics and astrophysics
RD9	W.B. Doriese et al.	LTD-13 AIP Conf. Proc. 1185, 450-453 (2009)	Optimal filtering, record length, and count rate in transition-edge-sensor microcalorimeter
RD10	P. Peille	pdf file sent per email, 13-06-2016	Mirror defocus, Impact on the X-IFU count rate capability, Preliminary results
RD11	C. Kilbourne et al.	Proc. SPIE 7011, June 2008	Multiplexed readout of uniform arrays of TES X-ray microcalorimeters suitable for Constellation-X

Abbreviations and acronyms

Item	Meaning
AHEAD	Integrated Activities for the High-Energy Astrophysics Domain
CSIC	
LPA	Large Pixel Array
SRON	SRON Netherlands Institute for Space Research
SPA	Small pixel array
TBC	To Be Confirmed
TBD	To Be Determined / Defined
TLA	Three Letter Acronym
VTT	
X-IFU	X-ray Integral Field Unit



WP6 X-ray sensor trade-off

Doc. no. : AHEAD-WP6-REP-002-2016

Issue : 1.1

Date : 16 September 2016

Cat :

Page : 5 of 23



WP6 X-ray sensor trade-off

Doc. no. : AHEAD-WP6-REP-002-2016
Issue : 1.1
Date : 16 September 2016
Cat :
Page : 6 of 23

1 Introduction

In this report we present the trade-off analysis performed for the X-IFU sensor. As part of the process to optimize the X-IFU sensor various options are available. During the trade-off some of these options were compared and the optimal route forward has been defined. Production of devices such as the development of Mo/Au TES (at CSIC) in addition to the Au/Ti (in SRON) is ongoing but isn't part of the trade-off (will be reported at the next stage). The trade-off included a detailed analysis of various sensor configurations taking into account the capability of the Athena mission. A new aspect in the mission is an active focussing mechanism. Using this and going to off-focus positions has for certain science cases a clear advantage (also over different pixel configurations) and this changes the optimizations considerable.

Before presenting the relevant instrument requirements and the trade-off of different options (section 2 and 3) we give in the introduction the WP description from the AHEAD consortium proposal (AD1: Call H2020-INFRAIA-2014-2015, proposal SEP-210187231) and the decision of the consortium board (AD2: AHEAD-PO-MIN-001/2015) as this provides the context. Following the trade-off we present an alternative approach (defocussing of the mirror in section 4) followed by the conclusions of this trade-off (section 5). In the appendix we give some progress on the fabrication of the devices, formally not part of the trade off report.

The AHEAD proposal lists under WP 6.2 the following for the X-ray sensors:

WP 6.2 X-ray sensors:
(SRON, CSIC, Lancaster)

Currently the baseline array is foreseen to include 3840 separate pixels, consisting of a TES and an absorber. The size of the absorbers is limited by the heat capacity and thermal conductivity of the Cu layer to about $250 \times 250 \mu\text{m}^2$ to meet the energy resolution requirement. This limitation, together with the maximum number of pixels which can be multiplexed in a single chain and the acceptable heatload on the cryogenic detector limits the Field of View to 5 arcmin and the maximum countrate to the equivalent of 10 mCrab (~ 50 counts/sec/pixel). If various sized absorbers can be implemented and multiple absorbers can be connected to a single TES, the limitations of the baseline array will be significantly relieved. It will allow a larger Field of View, combined with smaller pixels which do not undersample the mirror point spread function, have a better energy resolution and can sustain higher count rates without pile-up effects. In practice, not all these improvements will be achieved at the same time but a combination of different improvements is the likely outcome. The first part of this work package is to produce different absorbers/TES combinations and demonstrate their performance. Essentially, a number of parameters will be varied: the size of the absorber, the thickness of the Cu layer of the absorber and the thermal links from the absorber to the TES and from the TES to the bath. In addition different absorbers will be connected to a single TES using different thermal links. Using the shape difference in the pulses will allow us to identify the absorber which is hit by the photon. In this way the number of pixels can be increased by a factor 4 or more for the same thermal and readout conditions.

Another parameter that can be varied is the material of the bilayer in the TES. So far different bi-layers have been used for the TES (Ti/Au and Mo/Au) resulting in different results, but also tested in different test setups by different groups. Compared to Ti/Au, traditionally used by SRON, Mo/Au TESes have a higher volume which facilitates thermalization, and decreases the requirements on the Cu thermalization layer. These properties might allow for the design of larger pixels, without losing energy resolving power. Simultaneously, Mo/Au also has a higher heat capacity per unit of X-ray stopping power, which lowers the theoretical pixel size with respect to TiAu TESes. Manufacturing and material properties will ultimately



WP6 X-ray sensor trade-off

Doc. no. : AHEAD-WP6-REP-002-2016
Issue : 1.1
Date : 16 September 2016
Cat :
Page : 7 of 23

determine what is the optimal combination, and both routes will be explored in this work package. The second part of this work package is to compare the performance and understand the underlying physics between these different sets of bilayers. The objective is to simulate thermodynamic and transport properties of proximised Ti/Au and Mo/Au bi-layers, better understanding of electrostatics of weakly superconducting TESs under DC and AC bias and energy transport beyond discretised lumped element approach if necessary. Based on this comparison the best possible TES can be designed and this will be a second route to optimize the detectors. For these steps we will use existing production facilities at SRON and in Spain for the production of the baseline sensors, and the theoretical expertise present in Lancaster to analyse the performance of the detectors and to explore new combinations of properties and physical processes to enhance performance.

At the first board meeting it has concluded to shift some of the emphasis from the detector to the read-out as this is a very critical subsystem. In addition it was concluded at the start of the project that some of the options are less critical than others, taking into account the planned observations with the Athena mission. More specific it was concluded that the spectral resolution and high countrate capability had clear priority over a larger field of view and therefore detailed studies of the so-called hydra pixels had no priority anymore (see below for the board decision).

The board was informed about developments in optimizing the detectors for Athena which were carried out between the AHEAD proposal and the kick-off. This work has been performed in the Athena X-IFU program development which started its activities around the submission of the AHEAD proposal. The goals of the detector work package (WP6) remain unchanged but some of the trades have been performed in the context of the X-IFU and this will be taken into account. Therefore the following two changes are proposed:

- (a) the emphasis for the development of the detectors is the read-out and not the hydra pixels (based on recent analysis spectral resolution and count-rates have priority over a larger field of view with poorer resolution and additional under-sampling) (WP6.2)*
- (b) The optimization of the readout is not limited to the temperature levels of the electronics and SQUID dynamic range but will include a broader range of options (WP 6.3)*

The deliverables and milestones remain unchanged.

The relevant deliverable addressed in this report is given below [AD1]:

Num ber	Name	Short name	Type	Dissemi- nation level	Delivery date	expectation
6.1	Design trade off report: X-ray sensors	SRON	R	CO	12	SRON-ESA-CTP-TN-2016-01, page 3-15 but future improvements are expected based on test results

It should be noted that this work is closely related to the optimization of the X-IFU detector and as such, information from the development of this instrument is used. The focus of the trade-off is to identify the best possible direction of the sensor development in AHEAD to enhance the performance.



WP6 X-ray sensor trade-off

Doc. no. : AHEAD-WP6-REP-002-2016
Issue : 1.1
Date : 16 September 2016
Cat :
Page : 8 of 23

2 Transition Edge Sensors for detecting X-rays

2.0 Detection principle

A detailed description of the instrument is given in [RD4]. For ease of the reader we present in this section the basic detection principle for this type of detectors.

The TES micro-calorimeter senses the heat pulses generated by X-ray photons when they are absorbed and thermalized (see Figure 1). The temperature increases sharply with the incident photon energy and is measured by the change in the electrical resistance of the TES, which must be cooled at a temperature around 50 mK and biased in its resistive transition between the superconducting and normal states (Irwin and Hilton, 2005, and references therein). The absorber is composed of a layer Au and a Bi to achieve the correct stopping power at 6 keV and low heat capacitance required for high energy resolution. We plan to explore both Mo/Au and Ti/Au bilayer TES for the X-IFU.

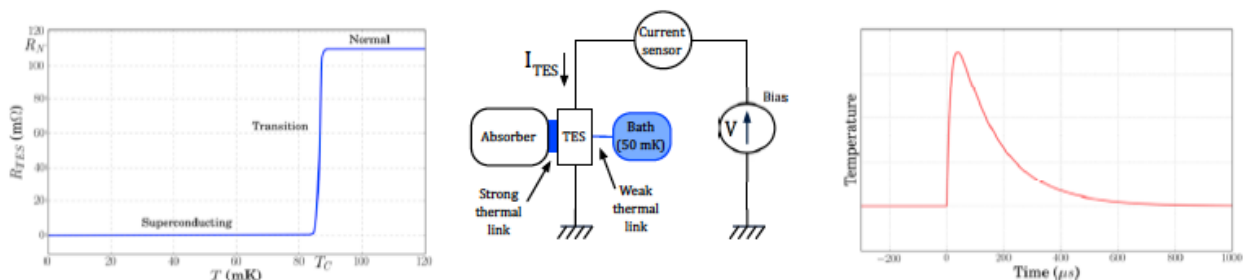


Figure 1. Principle of a TES (Transition Edge Sensor) acting as a micro-calorimeter. Left panel: The TES is cooled to lie in its resistive transition between its superconducting and normal states. Middle panel: The absorption of an X-ray photon heats both the absorber and the TES through the strong thermal link. Right: The change in temperature (or resistance) with time shows a fast rise (due to the strong link between the absorber and the TES) and a slower decay, governed by the ratio of the heat capacity C and the conductivity G to the thermal bath, but speeded up by roughly an order of magnitude using negative electro-thermal feedback.

2.1 Spectral resolution

The most demanding requirement on the X-IFU instrument is on the spectral resolution, which is required to be at or below 2.5 eV (FWHM) for the energy range 0.2 - 7 keV. This is a requirement at instrument level, which implies that apart from the intrinsic spectral resolution of the sensor array other contributions must be taken into account. A breakdown of the energy resolution budget, with a justification and a breakdown of requirements at engineering level is provided in RD6. A top-level summary of the budget is provided in Table 1. The main contribution to the 2.5 eV comes naturally from the sensor array: 1.9 eV has been reserved for the intrinsic energy resolution of the detector, which includes phonon and Johnson noise, effects from non-linearity and, possibly, excess noise. Contributions other than noise come from the array environment (thermal crosstalk and cosmic ray impacts on the wafer), non-optimal operating point, and energy resolution degradation due to dependence of measured energy on the photon absorption location in the absorber. They add up to a reservation of 1.94 eV. The remaining 1.58 eV is specified in the Table, and comprises all contributions to the signal line from the array to and including the event processing unit.

Different types of contributions are distinguished:

- **Noise terms.** Typically in a unit per $\sqrt{\text{Hz}}$. Add in quadrature. The noise bandwidth is determined on the low frequency end by the length of an event and on the high frequency end by the information bandwidth of the detector (after optimal filtering).



WP6 X-ray sensor trade-off

Doc. no. : AHEAD-WP6-REP-002-2016
Issue : 1.1
Date : 16 September 2016
Cat :
Page : 9 of 23

- *Gain drift terms.* Typically in rms unit per length of time. Represent the residue of gain drift after gain calibration, using events from the calibration source. The bandwidth is determined on the high frequency side by the event length and on the low frequency side by the time it takes to collect sufficient calibration events to perform the gain calibration to the desired accuracy. It is assumed that the various drift terms in the budget are independent and thus add in quadrature.
- *Other terms* (or noise terms that cannot be expressed in unit per $\sqrt{\text{Hz}}$, or gain drift terms that cannot be expressed as rms unit per length of time), include shot noise contributions (low-E photons, cosmic rays, crosstalk, microphonics, computational errors) and gain terms (positional dependence in absorber of measured energy).

Table 1. The spectral resolution budget for the flight model X-IFU instrument.

Contribution	Total	Noise	Drift	Other	Comment
Sensor array	1.94	1.90	0.00	0.41	Includes effect of biasing detector, comic ray hits and cross talk at highest countrates
Focal plane assembly	0.61	0.42	0.14	0.41	Includes cold electronics, cryoAC, filters Excluding sensor array
Digital electronics	0.79	0.77	0.17	0.02	Dominated by DAC performance
Detector cooling system	0.63	0.40	0.40	0.28	Including aperture cylinder and harness
Warm Front-End Electronics	0.42	0.28	0.30	0.10	
Engineering Margins	0.71	0.41	0.41	0.41	
Instantaneous gain calibration uncertainty			0.10		Residual uncertainty after calibration source events are used to calibrate gain scale
Root-sum square subtotal		2.19	0.69	0.78	
Finite record length		2.28			Consistent with a 4% degradation of resolution. Applies to noise sources only.
Total energy resolution	2.50				At instrument level

2.3 Count rate

Another important aspect of the detector is its count rate capability, in particular in combination with achieving a high energy resolution, for point sources. Point source strengths are commonly expressed by astronomers in units of Crab. One Crab is equal to the flux received from a point source with the same strength as the Crab Nebula in the energy range from 2.5 to 10 keV, with a Crab spectrum, assumed to be a power law of index 2.1, a normalization of 9.5 photons/cm²/s/keV and a column density of $4 \cdot 10^{21}$ cm⁻². Such a spectrum produces about 94000 counts/s on the TES array. The key metric for count rate requirement is throughput, defined as the fraction of photons absorbed by TES pixels for which an energy measurement is achieved above a certain grading. Valid events fall into three grading categories, which are based on the time intervals between the arrival of a photon and the preceding and succeeding photons per pixel. Close succession of photons hampers the accurate determination of the energy in the pulse processing. The three grading categories are specified for the baseline detector in RD7 as follows:

Table 2. Definition of event grading, cf. RD7

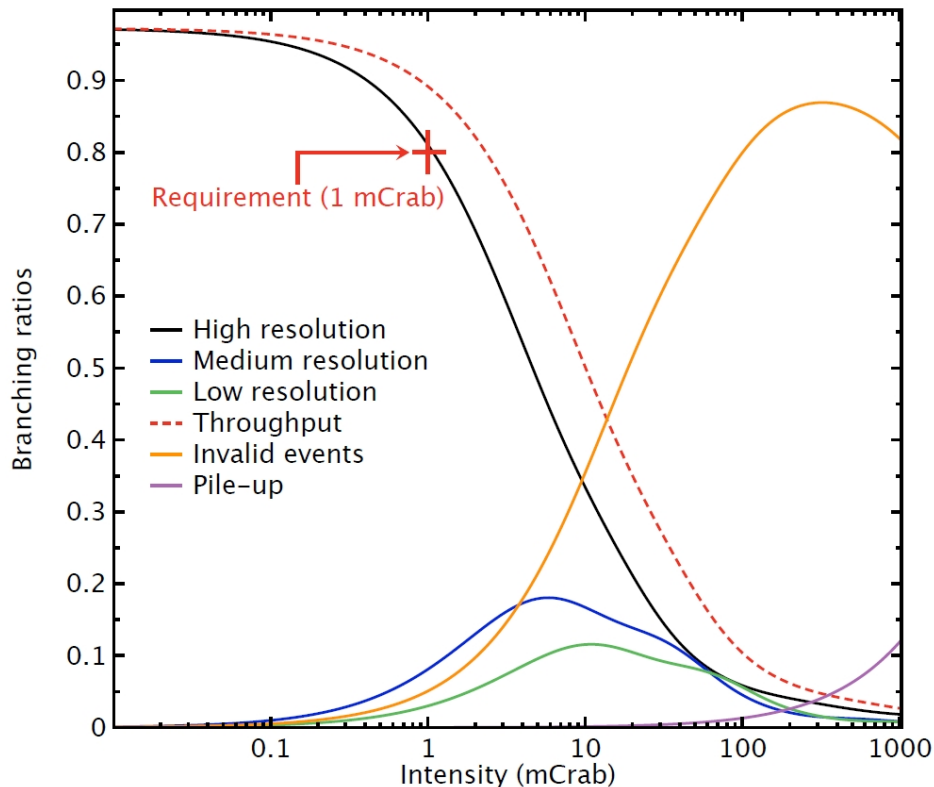
Grade	Time until next pulse	Time since previous pulse	Energy resolution
High resolution	≥ 6.6 ms	≥ 2.6 ms	2.5 eV
Medium resolution	≥ 1.6 ms	≥ 2.6 ms	3 eV
Low resolution	≥ 6.4 μ s	≥ 2.6 ms	15 eV
Pile-up	-	≥ 2.6 ms	-



WP6 X-ray sensor trade-off

Doc. no. : AHEAD-WP6-REP-002-2016
Issue : 1.1
Date : 16 September 2016
Cat :
Page : 10 of 23

The driving requirement for count rate capability in combination with energy resolution is the requirement to observe a 1 mCrab point source with an 80% throughput of 2.5 eV events. *Figure 2* shows the distribution of event grading over the above categories as a function of point source intensity for the baseline detector. It shows in particular that the detector is capable of meeting the count rate requirement.



4 *Figure 2. The distribution of the different event grades for the baseline configuration of the X-IFU TES array (based on the LPA1 pixel design) as a function of point source intensity. Event grading is based on the time interval between the preceding and succeeding pulse, with "high resolution" corresponding to conditions promoting ≤ 2.5 eV. The throughput is given as the sum of all valid events. The invalid events are rejected. The pile-up fraction is also shown and starts increasing above 100 mCrab (the sampling frequency is 156 kHz). The (LPA1) baseline pixel design was defined to match the count rate requirement of 80% of high-resolution events at 1 mCrab (indicated by a red cross).*



WP6 X-ray sensor trade-off

Doc. no. : AHEAD-WP6-REP-002-2016
Issue : 1.1
Date : 16 September 2016
Cat :
Page : 11 of 23

3 Instrument requirements

The prime instrument requirements are given in Table 3. For each of the requirements we identify where it affects the detector optimization and/or other parts of the instrument. As can be seen some parameters have direct impact on the sensor, whereas others define other parts of the instrument electronics.

Table 3. Overview of the driving instrument requirements (X-IFU)

Parameter	Value	Comment
Effective area	1.43 m ² at 1 keV and 0.24 m ² at 7 keV	This parameter forms the basis of the assessment of the scientific performance of the Athena/X-IFU instrument. It is a combination of the optical and detector detection efficiencies. The detector detection efficiency itself can be broken down in the transmission through the thermal/optical filters, the filling factor of the detector plane, the fraction of working pixels and the fraction of events with good spectral resolution. For the sensor the optimization should therefore be: <ul style="list-style-type: none"> - filling factor of the detection plane determined by achievable pixel to pixel separation and space needed for the stripline wires - fraction of working pixels (close to 1) - fraction of events with good spectral resolution (depends on the speed of the detector and the required countrate capability)
Quantum efficiency	70% at 7 keV and 60% at 1 keV	Part of the detector contribution to the effective area. At higher energies the thermal/optical filters in the detector are essentially 100% transparent and the detector efficiency is determined by the stopping power (thickness) of the absorbers. The stopping power is mainly determined by the thickness of the Bi layer in the absorber. The Bi does hardly contribute to the heat capacity. At lower energies the stopping power is essentially 100% and the QRE is driven by the transparency of the optical filters.
Fill factor	≥ 90%	Part of the detector contribution to the effective area. This requirement drives the ratio between the absorber size and the space between absorbers. The minimal space between the absorbers is again driven by the thickness of the absorber, which is driven by the quantum efficiency requirements.
Spectral resolution	2.5 eV up to 7 keV, E/ΔE = 2800 above 7 keV 1.5 eV (goal)	This is the most demanding requirement on the X-IFU together with the number of pixels. The intrinsic detector energy resolution is given by: $\Delta E = 2.355 (0.5n)^{1/4} \text{ sqrt}(4 kT^2 C/\alpha)$ and as such is determined by the phonon transport n , the critical temperature T , the heat capacity C and the TES sensitivity $\alpha = T/R \text{ dR/dT}$. The heat capacity is mainly provided by the Au or Cu layer in the absorber. With a TES-based detector, a ΔE near 2 eV is realistic for pixels in the range between 100 x 100 to 300 x 300 mm ² . However, it should be noted that the instrument resolution is not only determined by the intrinsic properties of the sensor but also include contributions from the read-out chain as has been discussed in section 2.2.



WP6 X-ray sensor trade-off

Doc. no. : AHEAD-WP6-REP-002-2016
Issue : 1.1
Date : 16 September 2016
Cat :
Page : 12 of 23

		It should be noted that the goal of 1.5 eV is ambitious.
Energy range	0.2 – 12 keV	The energy range determines mostly the properties of other systems such as the transmission in the optical/thermal filters at the low end and the dynamic range of the read-out system of the detector on the high side and as such is of secondary relevance. It should be noted that lowering the upper bound of this range (or requiring less spectral resolution) will make the prime requirement of a ΔE of 2.5 eV slightly easier.
Field of view	5 arcmin (diameter)	The field of view allows the efficient observations of spatially extended sources. This is mainly restricted to nearby clusters of galaxies and Supernova Remnants. Based on the Athena Mock Observing Plan (RD5) the number of related observations is limited (< few% of the observing time). Therefore it has been judged that optimizing the detector for the other parameters (energy resolution and handling higher count rates) is the preferred emphasis. A larger Field of View would also imply a larger detector assembly and based on the current resource budgets for Athena, the instrument is already mass limited due to its dewar. Hence, a larger Field of View is not compatible with the instrument resources.
Count rate capability	<p>1 mCrab with >80% high resolution events</p> <p>1 Crab with >30% throughput of valid events but 30 eV resolution only</p>	<p>To allow the detection of weak emission or absorption features in the spectra of bright sources, it is required that a large fraction of the events has a resolution of 2.5 eV or better and are sufficiently isolated from preceding and subsequent events to allow the event processing to obtain this high resolution. These are the so-called high resolution events. The driving science for this is to detect imprints of the Warm Hot Intergalactic Medium in the afterglow of a Gamma Ray Burst.</p> <p>Different options to reach this capability have been identified during the trade-off studies:</p> <ul style="list-style-type: none"> - a special sub-array (called Small Pixel Array) can be adjusted to optimize the count rate capability - defocussing the mirror (see section 5) would make this requirement easy to meet or even to be much better (close to 100%) <p>The requirement for very bright sources defines the capability to process and store events onboard including the need for interchangeable external filters (e.g. a neutral density filter) and does not directly affect the sensor optimization</p>
Non X-ray background	$< 5 \cdot 10^{-3}$ counts/cm ² /keV	This is achieved by an active anti-coincidence detector and part of another AHEAD work package (6.3) and therefore not addressed in this trade-off.



WP6 X-ray sensor trade-off

Doc. no. : AHEAD-WP6-REP-002-2016

Issue : 1.1

Date : 16 September 2016

Cat :

Page : 13 of 23

4 Defocusing optics

Recently a hexapod system has been selected for the Athena mission. By rotating the mirror in the telescope either the WFI or the X-IFU can be selected. This is illustrated in Figure 3. Allowing a somewhat larger stroke on the hexapod, the image of a strong point source can be distributed over a larger number of pixels, relaxing the count rate requirement considerable. This is shown in Figure 4 where the image is diluted over a larger number of detector pixels if the instrument is placed out of focus between 0 mm and 40 mm (on a focal length of 12 m).

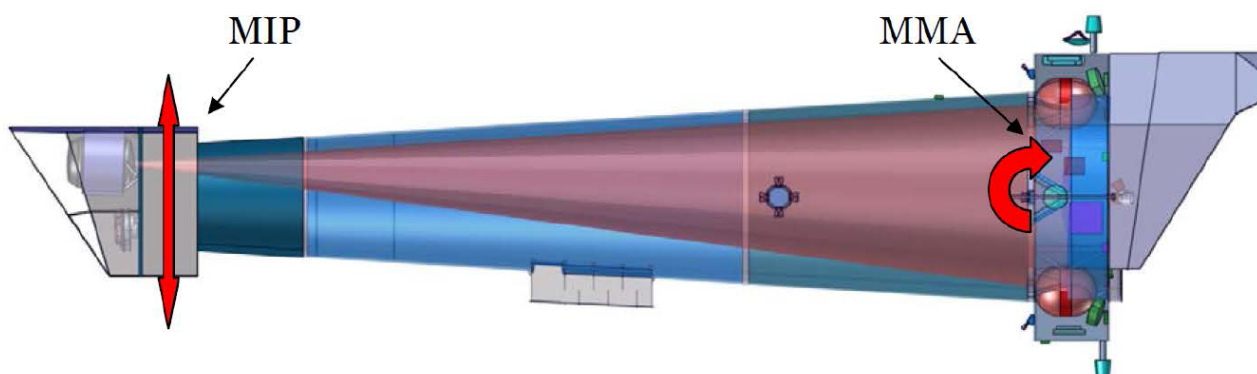


Figure 3. Athena satellite with the two instruments on the left and the mirror Module Assembly (MMA) on the right. Selection of the instrument is illustrated by the purple cone and the instrument is selected by rotation of the MMA.

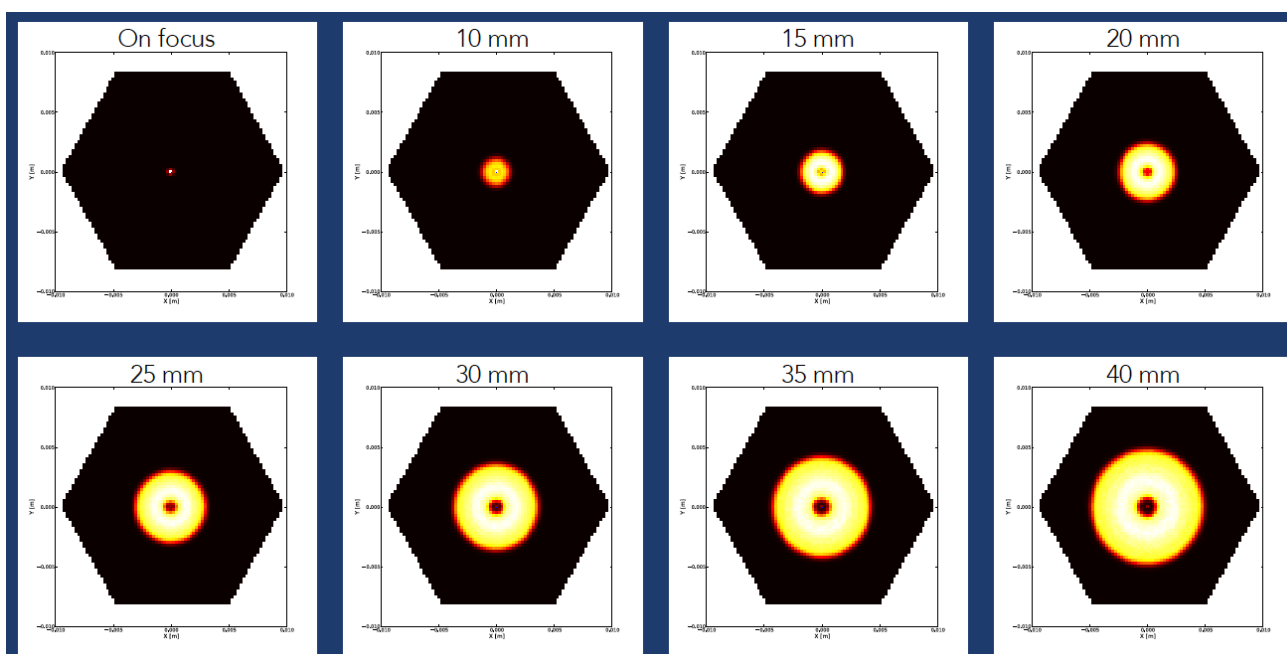


Figure 4. Effect of defocusing on a point source. For strong sources the background is relatively unimportant.



WP6 X-ray sensor trade-off

Doc. no. : AHEAD-WP6-REP-002-2016
Issue : 1.1
Date : 16 September 2016
Cat :
Page : 14 of 23

Essentially this allows the reduction of the count rate on a single pixel to a value consistent with bright extended sources and removes the necessity for fast pixels or small pixels to achieve a higher countrate. Below we summarize the advantages of such system and define the direction for future sensor development.

4.1 Simpler array fabrication

Compared to its alternative - a hybrid array with LPA and SPA pixels - the defocusing option allows in principle the baseline option of a homogeneous array with one single version of pixels. The advantages pertain to the TES as well as the absorber. Although hybrid arrays have been demonstrated to be feasible, the fabrication risks and yield issues are expected to be larger.

4.2 Simpler array wiring

Having less pixels in the center of the array lowers the wiring density in the entire array. Since the pixels could be of the size 260 - 300 μm without hardly any penalty for confusion noise (RD1, p. 37), the routing of the wiring across the array becomes easier, further lowering fabrication risks.

4.3 Relaxed readout requirements

The required number of readout chains scales roughly with the number of pixels times the required bandwidth per pixel. Hence the requirements on the readout resources might be relaxed for several reasons:

- When the SPA is discarded altogether, the field-of-view is tiled with a minimum number of pixels
- As the counts from the high flux point sources are spread over a large number of pixels, the required countrate per pixel drops, allowing lower bandwidth pixels. Figure 5a and b show the throughput of high-resolution events as a function of the strength of a point source, for different levels of defocussing, for two types of detector under consideration for implementation in the TES sensor array. Both detectors allow the requirement to be met for 1 mCrab when 10 mm defocus is possible, and the goals to be obtained when 30 to 35 mm defocussing is possible.
- One might still consider to have an SPA with a relaxed count rate requirements for the pixels, to allow the study of point sources with a Nyquist sampled PSF. This decision can be made later, as these studies are not part of the core science.

4.4 Longer event lengths

One further advantage of lowering the count rate per pixel is that the same high-resolution throughput can be met with longer event lengths. The longer the event length, the lower the impact on the resolution degradation due to integrated noise on the baseline determination. This process is described in detail in RD9. In the current energy resolution budget a penalty of 4% on the noise terms is allocated. E.g., reducing this term by a factor of 2 would allow an extra (root sum square) margin of 0.45 eV. It is a trade between defocus level and high-resolution throughput that will determine the extra margin in the resolution budget.

4.5 Uniform calibration counts

An array with uniform pixel sizes will not suffer from the problem of non-uniformity of the calibration counts, that is an issue with the hybrid array. Relative to the LPA pixels, the SPA pixels will receive 0.4 to 0.1 of the calibration photons under normal illumination, which make the calibration of the SPA pixels dependent on a considerable level of coherent drifting in the SPA.

4.6 Less (thermal) crosstalk

Thermal crosstalk is hugely reduced when the count rates in adjacent pixels drop. In high countrate circumstances, thermal crosstalk appears a dominant contributor to the offset of measured energy for source strengths above ~ 1 mCrab. Spreading the photons over a larger number of pixels reduces the thermal



WP6 X-ray sensor trade-off

Doc. no. : AHEAD-WP6-REP-002-2016
Issue : 1.1
Date : 16 September 2016
Cat :
Page : 15 of 23

crosstalk. As this also means that the counts will be spread across a larger number of readout chains, the chances for other types of crosstalk are also reduced.

4.7 Relaxed pointing requirements

As the SPA under consideration only measured about 30" x 30" in size, strong point sources need to fall inside a smaller area (at most 20" x 20") in order to prevent appreciable loss of high quality counts. This puts stringent requirements on the Line-of-Sight Absolute Performance Error (APE) and Performance Drift Error (PDE), of the order of 10" (defined as a 95% confidence interval). These requirements can be relaxed for the observation of strong point sources in the case of defocusing as the size of the Half Energy Width (HEW) is enhanced with respect to the APE and the PDE, and the relative size of the sensitive area becomes ~10 times larger (from 30" to 5').

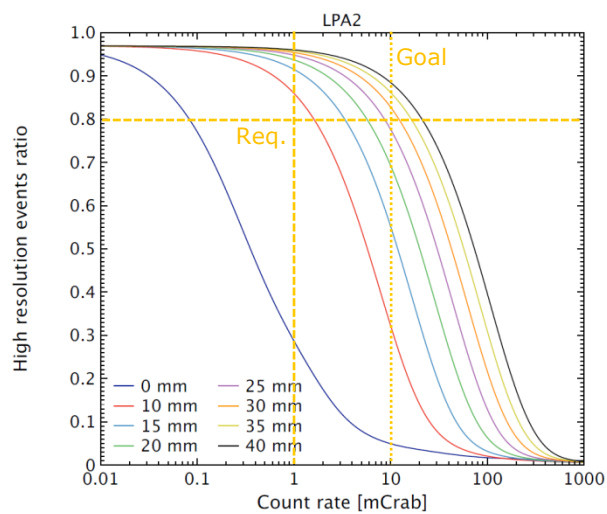
4.8 Uniform loading of readout chain

A large HEW compared to the pointing error also implies that the defocused PSF will appear in the center of the array for every observation. With readout chains that are wired to contain 'pie-slices' of pixels, a bright source exposure will more or less equally load each readout chain in the array. This makes optimal use of the available pulse processing and other readout resources, and thus requires the smallest margin on individual processors and other components.

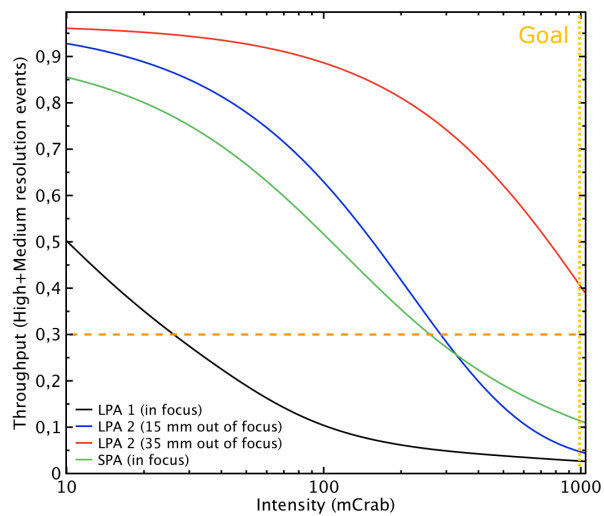


WP6 X-ray sensor trade-off

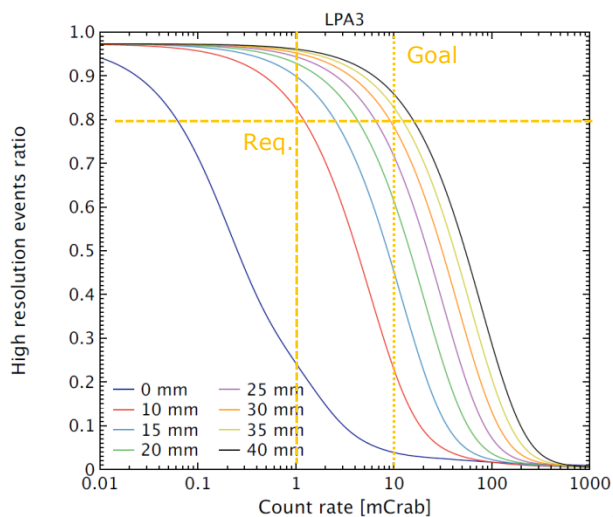
Doc. no. : AHEAD-WP6-REP-002-2016
Issue : 1.1
Date : 16 September 2016
Cat :
Page : 16 of 23



a.



b.



c.

Figure 5. Fraction of high-resolution events after event grading (pile-up detection) as a function of point source strength, for different values of mirror defocussing (adapted from results with the SIXTE end-to-end simulator presented in RD10) a. Throughput as function of count rate for a GSFC LPA2 detector with an information bandwidth (effective frequency, cf. RD9) of 550 Hz. Orange lines indicate the instrument requirements and goals. b. Throughput of high and medium resolution events for LPA1 and SPA detectors in focus, and LPA2 for two defocussing values in the context of the observation of a 1 Crab point source. c. Throughput as a function of count rate for a detector twice as slow as LPA2, showing further room for advancement of the detector design.



WP6 X-ray sensor trade-off

Doc. no. : AHEAD-WP6-REP-002-2016
Issue : 1.1
Date : 16 September 2016
Cat :
Page : 17 of 23

5 Sensor trade-off

Optimization of the sensor can be done in many different ways. We have selected five basic options for the trade off, taking into account all other boundary conditions:

- LPA1: a uniform array with a relatively fast detector provides the required point source count rate capability over the full detection plane, but at the expense of a stronger demand on the read out resources.
- LPA2: with a factor 2 slower detector the intrinsic count rate capability is lower but the requirements on the read-out chain and detector are easier to be met. In combination with defocusing of the optics this is an attractive option. This detector is close in design to detectors currently being tested in the laboratories, so it also requires a minor development effort.
- LPA3: this detector would be another factor 2 slower, making a proportionally lower demand on readout bandwidth, and would still meet the goal of reading out a 10 mCrab point source with 80% throughput at high resolution (Figure 5c). The lower bandwidth is achieved by modifying the conductivity G to the thermal bath, as raising the heat capacity C would negatively influence the energy resolution.
- LPA2 + SPA1/2: in the somewhat slower detector array a dedicated array with smaller pixels can be placed in the center (blue box in Figure 6). This dedicated array can be optimized for higher count rates, a better sampling of the mirror PSF or a better energy resolution. This array is also called a hybrid array.

Table 4 summarizes design parameters for different options for LPA and SPA pixels.

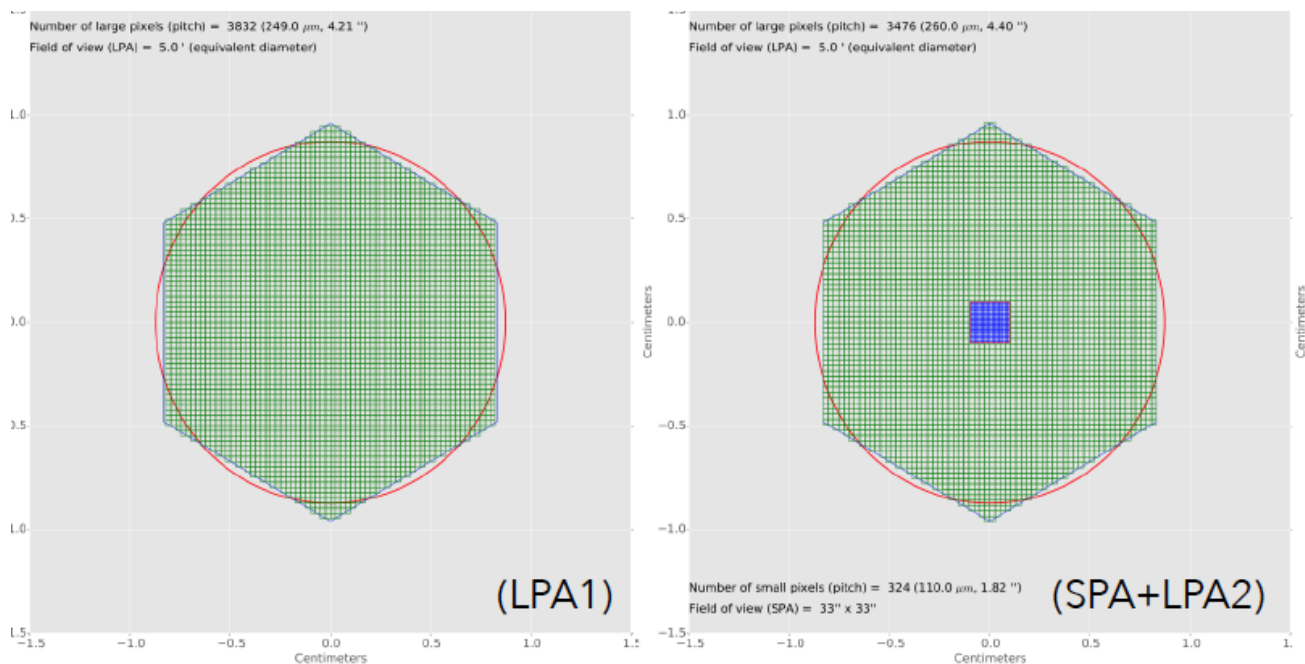


Figure 6. Options for the sensor configuration



WP6 X-ray sensor trade-off

Doc. no. : AHEAD-WP6-REP-002-2016
Issue : 1.1
Date : 16 September 2016
Cat :
Page : 18 of 23

Table 4. Typical parameters for the different possible pixel designs. Based on GSFC information for Mo/Au-based TES pixel and processing, but apply to Ti/Au-based TESs as well.

Parameter	LPA1	LPA2	LPA3	SPA1 Improved count rate	SPA2 Improved ΔE
Pixel size	250 μm	250 μm	250 μm	100 μm	75 μm
Power	4.6 pW	2.7 pW	1.3 pW	5.8 pW	-
Critical temperature	90 mK	90 mK	90 mK	90 mK	58 mK
Heat capacity	0.8 pJ/K	0.8 pJ/K	0.8 pJ/K	0.25 pJ/K	-
Heat conductivity to bath	200 pW/K	115 pW/K	57 pW/K	300 pW/K	-
ΔE FWHM @ 6 keV	1.74 eV (model)	1.73 eV (model)	1.72 eV (model)	1.58 eV (model)	1.56 eV (meas.)
ΔE FWHM @ 1.5 keV	~ 1.74 eV (est.)	~ 1.74 eV (est.)	~ 1.72 eV (est.)	~ 1.58 eV (est.)	0.87 eV (meas.)
Effective bandwidth	960 Hz	550 Hz	275 kHz	1.7 kHz*	~ 1 kHz

Based on these design parameters, which are challenging but realistic, a trade-off is presented in Table 5.

A uniform array of LPA1 pixels, which served as a baseline until recently, would allow us to meet the requirements of 2.5 eV resolution for a 1 mCrab point source. It is based on demonstrated technology (RD11). This option has the disadvantage of demanding quite substantial read out resources, as all read-out channels are equally dimensioned whereas the high count rate is limited to a few pixels only. Given the pointing accuracy of the telescope, bright point sources can be accurately located close to the center of the array, so a large fraction of the required bandwidth is never used in this option.

There are two optimizations on this option possible:

1. In combination with defocusing of the optics, as discussed in the previous Section, a uniform array of slower pixels would be a good solution. Effectively, defocusing turns bright point sources in much less bright extended sources, such that the bandwidth that is needed to observe focused extended sources, which are part of the Athena science program anyway, is also sufficient for the point sources. LPA2, as defined in Table 4, is a detector that provides a clear saving in readout resources, while at the same time allowing to reach the goal of observing 10 mCrab point sources with 80% high-resolution throughput. As is illustrated in Figure 5c, the detector could even be slowed down a further factor of 2, which is LPA3, and still be compatible with this goal. LPA2 has the advantages of facilitating another goal, the observation of 1 Crab extremely bright sources with a >30% throughput of valid events, and being very close in design to detectors currently being tested in the laboratories. In that respect LPA2 offers a realistic option, whereas a further slowed-down LPA3 pixel requires additional research effort with the associated risk.
2. Instead of defocusing, another option is the application of a Small Pixel Array in the centre of the LPA2, which is optimized for a higher count rate. This option has also the potential of reaching the 10 mCrab point source goal. Compared to the defocusing option this option has a few down sides. First, a hybrid array is more complex to fabricate than a uniform array, and although GSFC has demonstrated hybrid array technology, there are associated risks which may impact on yield and uniformity. Second, this option does not allow obtaining the 1 Crab goal. Third, this option effectively replaces 36 low-bandwidth LPA2 pixels by 324 high-bandwidth SPA1 pixels, so although it provides a considerable saving on read out resources compared to the uniform LPA1 array, it requires more resources than the uniform LPA2. In principle, defocusing results in a relatively higher background and reduced imaging capability, but for bright point sources the background is not critical, and the level of defocusing can be adjusted to the source strength so that per source a trade between imaging and count rate capability is possible.



WP6 X-ray sensor trade-off

Doc. no. : AHEAD-WP6-REP-002-2016
Issue : 1.1
Date : 16 September 2016
Cat :
Page : 19 of 23

Another enhancement of the LPA2 array would be an SPA2 array optimized for better energy resolution at lower photon energies. At single pixel level an energy resolution of 0.7 eV has been demonstrated at an energy of 1.5 keV (RD8), which would result in an energy resolution of ~ 1.7 eV at instrument level if no improvements are made to the read-out chain. This improvement would provide a significant advantage in the detection of weak absorption lines.

The performance of such small pixels has been experimentally verified on an individual level in RD8. Combining such pixels in a hybrid array with LPA2 pixels poses significant additional technical challenges, given the difference in critical temperature of the LPA2 and SPA2 pixels, the differences in substrate and the need to develop an alternative heat sinking layer, the required low heat capacity of this SPA2 pixel, which imposes limits on the absorber volume. It remains therefore to be seen to what extent the excellent resolution demonstrated at single-pixel level RD8 can be realized in a hybrid array setting. Also the highly non-linear response of the device poses a challenges. While it allows a better energy resolution at lower energies, obtaining good resolution at higher energies requires a more complex pulse processing which takes into account the non-linearity and non-stationary noise. The non-linearity will also make the gain calibration more cumbersome. Finally, the full advantage of higher spectral resolution is limited by two factors:

1. Unless the whole readout chain undergoes significantly improvement, it will contribute ~ 1.6 eV to the detector resolution (RD6) limiting the instrumental resolution at low energies to ~ 1.7 eV.
2. The area of the SPA2 is limited, so by higher defocusing levels a considerable fraction of the photons will fall outside the SPA2 (see Figure 4), limiting the advantage of the high resolution for weak line detection. The SPA2 has a considerable bandwidth, allowing a few tens of counts per second per pixel with a sufficient high- resolution throughput, so a trade needs to be made between the obtainable speed of the detector in a hybrid array and the required level of defocusing to obtain the required high-resolution throughput.



WP6 X-ray sensor trade-off

Doc. no. : AHEAD-WP6-REP-002-2016
Issue : 1.1
Date : 16 September 2016
Cat :
Page : 20 of 23

Table 5. Detector trade-off.

Device	Optimization	Pro	Con
Uniform array: LPA1	<ul style="list-style-type: none"> Count rates of 1 mCrab per PSF 	<ul style="list-style-type: none"> Modest modification to demonstrated technology 	<ul style="list-style-type: none"> High bandwidth demand on readout with no real science return
Uniform array: LPA2	<ul style="list-style-type: none"> Optimized for bright extended sources and defocused point sources 	<ul style="list-style-type: none"> Modest modification to demonstrated technology Allows countrate goals for 10 mCrab and 1 Crab point sources Enables larger Field of View or smaller pixels within the same read-out resources due to lower bandwidth requirements 	<ul style="list-style-type: none"> Higher background in defocused operation
Uniform array: LPA3	<ul style="list-style-type: none"> Optimized for bright extended sources and defocused point sources 	<ul style="list-style-type: none"> Lowest demand on read out resources. Allows goal for countrate of 10 mCrab point sources Enables larger Field of View or smaller pixels within the same read-out resources due to lower bandwidth requirements 	<ul style="list-style-type: none"> Additional development effort needed. Higher background in defocused operation
Hybrid: LPA2 + SPA1	<ul style="list-style-type: none"> Count rate 	<ul style="list-style-type: none"> Allows goal for countrate of 10 mCrab point sources and observation of diffuse halo around a these sources simultaneously (only a few sources have been defined) Improves sampling of the PSF 	<ul style="list-style-type: none"> Complexity of device, requiring substantial additional development. Larger demand on readout resources. No added value compared to defocusing option. Lower filling factor
Hybrid: LPA2 + SPA2	<ul style="list-style-type: none"> Energy resolution 	<ul style="list-style-type: none"> Allows goals for countrate of 10 mCrab point sources and Enhanced ΔE below 1.5 keV Improves sampling of PSF 	<ul style="list-style-type: none"> Extreme complexity of device, requiring large additional development effort. Different T_C's in hybrid array Highly non-linear detector: complex pulse processing and calibration. Absorber size limited by low C requirement In defocused mode, ΔE advantage is limited to a subset of the events. Larger demand on and limitation from readout. Lower filling factor



WP6 X-ray sensor trade-off

Doc. no. : AHEAD-WP6-REP-002-2016
Issue : 1.1
Date : 16 September 2016
Cat :
Page : 21 of 23

6 Conclusions

In this section we present the conclusions for the current trade-off analysis. Whereas funding for the baseline TES array will be funded as part of the X-IFU development scheme, the AHEAD program allows us to develop improved detectors based on Mo/Au or Ti/Au bilayers. Considering the Athena capability (defocusing which allows for higher count rates) and the limited number of extended sources requiring multiple pointings, the improvements on the current baseline will take place in the context of realising high count rate goals by utilizing the defocusing capabilities of the telescope. From the trade-off above we derive two recommendations for the AHEAD detector program:

1. In line with the decision of the board meeting, the prime direction of detector improvement will be geared towards a lower bandwidth requirement (slower detectors). If feasible this allows the reduction of the read-out resources or an increase of the field of view or smaller pixels within the same Field of View. This latter option could be very attractive if combined with somewhat better energy resolution (even modest improvements of a few tenths of eV will be very valuable).
2. Another direction, with lower priority, will be improvement of the energy resolution in a part of the array. This improvement, resulting in a hybrid array of LPA2 or LPA3 pixels with an SPA2, provides a considerable challenge in fabrication and development, but with the potential of realizing a significant improvement in science capabilities of the instrument.

6.1 Baseline TES array

For the European baseline detector the presented LPA2 is a good match between the complexity of the electronics and the countrate requirement which is driven by bright extended sources. Using the defocusing capability, high count rates can be achieved with excellent spectral resolution (almost all events at 2.5 eV) and an acceptable demand on read out resources.

6.2 TES array with lower bandwidth

A lower bandwidth pixel, similar to LPA3 in Table 4, with Ti/Au TESs, alleviates derived requirements on the read out chain, which can be translated into lower power, lower mass, and/or lower risk. In order to lower the bandwidth, a reduction of the heat conductivity to the bath is required, rather than an increase of the heat capacity, which would have a negative impact on the energy resolution. Creating a larger impedance for the phonon flow to the bath is usually achieved by either thinning the membrane on which the TES resides, or by cutting slots in the membrane. Both paths pose challenges in the fabrication process.

6.3 Improved energy resolution

A desirable enhancement of the array is to improve the spectral resolution in a selected area as this directly impacts the weak line sensitivity, with potentially large scientific benefits. This is a technically challenging option as was expounded in Section 5. Therefore this will be explored as far as this is feasible to do in parallel to the main improvement (section 6.2). (it should be noted that in a single production runs sensors with different geometries are produced and this enables some exploration of future directions without requiring major additional resources.